金属基陶瓷复合等离子弧堆焊层组织与耐磨性能

刘政军[1]，　宗　琳[1,2]，　孙景刚[1]，　慈洪钢[1]，　宋兴奎[1]

（1. 沈阳工业大学 材料科学与工程学院，沈阳　110023；
2. 沈阳化工学院 机械工程学院，沈阳　110142）

刘政军

摘　要：等离子弧堆焊镍基和钴基合金粉末时外加纵向磁场，对两种合金陶瓷复合堆焊层进行硬度和磨损试验及显微组织分析．结果表明，施加磁场时的堆焊层性能比无磁场作用的堆焊层性能高．钴基合金的最佳焊接电流和磁场电流分别为 160 A 和 3 A，此时堆焊层组织晶粒细化效果最明显；而镍基合金为 140 A 和 1 A，此时堆焊层 Cr_7C_3 截面的六角形陶瓷硬质相数量最多且均匀分布，说明 Cr_7C_3 硬质相的轴向平行方向一致，因而硬度和耐磨性最好．随着磁场电流的继续增大，由于电磁阻尼占主导地位，这两种合金的性能均下降．

关键词：等离子堆焊；陶瓷复合；组织；耐磨性

中图分类号：TG290　　文献标识码：A　　文章编号：0253－360X(2009)01－0017－04

0　序　　言

等离子弧堆焊处理可以在廉价钢材表面形成性能优良的结合层，所得到的亚稳态合金以其特有的耐磨性、耐蚀性、耐热性，达到降低材料成本、节约贵重金属材料、提高材料使用寿命的目的，已日益引起人们的关注．其中钴基合金粉末和镍基合金粉末等离子弧堆焊显示出良好的应用前景[1－3]．

电磁作用焊接技术是近年来完善起来的一种新的焊接技术，通过外加纵向磁场赋予焊接电弧大的刚性和稳定性，并由于磁压增高的结果，提高了弧柱中心的温度．通过电磁搅拌作用，对熔滴过渡、溶池金属流动、熔池的结晶形核及结晶生长等过程进行有效地干预．改变焊接熔池液态金属结晶过程中的传质和传热过程，从而改变晶粒的结晶方向，细化一次组织，减小化学不均匀性，减小偏析，提高焊缝的力学性能，降低气孔、裂纹等焊接缺陷[4]，在国外被称为“无缺陷焊接”．

课题采用在 20G 钢板表面进行钴基和镍基等离子粉末堆焊过程中，通过加入纵向磁场改善堆焊层硬质相的形态和分布，对两种粉末堆焊层组织和性能进行了研究．

收稿日期：2008－01－12
基金项目：辽宁省自然科学基金资助项目(20042025)

1　试验方法

堆焊基材为 100 mm×80 mm×12 mm 的 20G 低碳钢试板，以镍基和钴基自熔性合金粉末作为堆焊材料，其化学成分见表 1 和表 2．

表 1　钴基合金粉末成分(质量分数，%)

Table 1　Chemical composition of Co-based alloy powder

C	Si	B	Cr	Fe	W	Co
0.87	2.6	0.88	27.27	3.4	5.37	余量

表 2　镍基合金粉末成分(质量分数，%)

Table 2　Chemical composition of Ni-based alloy powder

C	Si	B	Cr	Fe	Ni
0.77	4.0	3.24	16.3	12.3	余量

利用等离子弧焊机在 12 mm 厚的低碳钢钢板上分别堆焊镍基和钴基合金粉末，堆焊层厚度为 3～4 mm，堆焊工艺参数见表 3．

利用 HRC －150 型洛氏硬度计测量堆焊层表面的宏观硬度；将测试完硬度的试块用电火花切割成尺寸为 50 mm×27 mm×11 mm 的标准试件，在湿砂橡胶轮磨损试验机上进行磨损试验，利用分析天平称量每次磨损后的质量损失，来评定堆焊层的耐磨性；利用 OLMPUS BX －6 型金相显微镜对堆焊层金属进行显微组织观察．

表 3 堆焊工艺参数

Table 3 Welding parameters

电源功率 P/kW	空载电压 U_k/V	焊接电流 I/A	电弧电压 U/V	电极直径 D/mm	电弧纵向移动速度 v/(cm·min^{-1})	电弧横向摆动频率 f/(次·min^{-1})	电弧横向摆动宽度 w/cm	电极距工件表面距离 h/mm
50	90	100~200	30	3.2	4~6	45	2.2	4

2 试验结果及分析

2.1 堆焊层的硬度及耐磨性分析

图 1 和图 2 分别是钴基合金粉末和镍基合金粉末在最佳焊接电流下其堆焊层硬度随磁场电流的变化曲线. 图 3 和图 4 分别是两种合金的耐磨性随磁场电流的变化曲线.

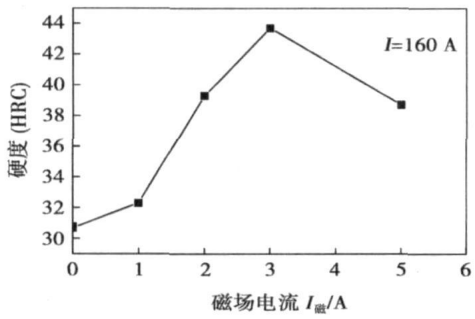

图 1 钴基合金堆焊层硬度随磁场电流变化曲线

Fig. 1 Variation of hardness with magnetic current for Co-based alloy

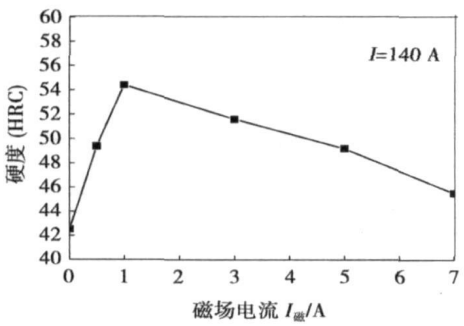

图 2 镍基合金堆焊层硬度随磁场电流变化曲线

Fig. 2 Variation of hardness with magnetic current for Ni-based alloy

从图中可以看出, 对于钴基合金, 最佳焊接电流为 160 A, 它所作用下的堆焊层在磁场电流 3 A 时硬度最高, 磨损量最小. 由于外加磁场促进了硬质相(碳化物 Cr_7C_3, 其形状一般为长条状, 截面为六角形)的形核, 磁场电流在3 A时, 堆焊层的显微组织

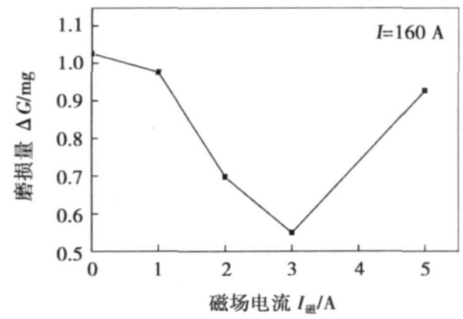

图 3 钴基合金堆焊层磨损量随磁场电流变化曲线

Fig. 3 Variation of wearing extent with magnetic current for Co-based alloy

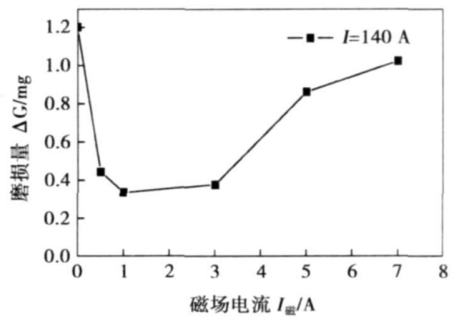

图 4 镍基合金堆焊层磨损量随磁场电流变化曲线

Fig. 4 Variation of wearing extent with magnetic current for Ni-based alloy

细化程度最大, 出现的硬质相数量最多且均匀分布; 从摩擦机理来说, 当硬质相成杆状垂直于被磨面时, 其材料受力较少, 故能提高表面的耐磨性[5]. 当磁场电流继续增大时, 堆焊层的硬度和耐磨性都在下降, 由于磁感应强度过度地增加, 导致一次组织粗大, 且出现了胞状树枝晶, 宏观上堆焊层性能下降. 对于镍基合金, 最佳焊接电流为 140 A, 磁场电流在 1 A 时硬度和耐磨性具有最佳值. 当磁场电流继续增大时, 堆焊层的硬度和耐磨性都在下降. 这是由于只有当焊接工艺参数和磁场强度相匹配时, 电磁搅拌起主要作用, 细化一次结晶组织, 改善堆焊层性能; 过大的磁场电流作用下, 电磁阻尼占主导地位, 抑制了熔体的自然对流, 因而抑制了热量的对流传输, 使温度起伏减少, 晶粒变得粗大, 堆焊层的性能

下降[6].

2.2　堆焊层的显微组织分析

图5 为最佳堆焊电流作用时, 磁场电流为 0, 1, 2, 3, 5 A 分别作用下钴基合金堆焊层表面的显微组织形貌.

可以看出, 钴基合金堆焊层的显微组织以奥氏体为主, 从显微形貌上可以清楚的看到大量的胞晶组织. 施加磁场后, 晶粒明显细化, 特别是磁场电流为3 A 时, 晶粒细化程度最大, 且分布均匀. 在一定的磁场强度范围内, 随着磁场电流的增加, 磁场强度增强, 作用于熔池的电磁力也随之增大; 熔池中的液态金属受洛仑兹力的作用, 绕焊接电弧中心轴旋转, 做复杂的循环运动, 磁场对熔池的搅拌作用也随之增强. 在离心力的作用下, 熔池前部高温液态金属被推向尾部, 结晶前沿的温度及温度梯度提高等因素的影响, 使得结晶前沿存在着较强的液相流动, 从而使枝晶折断; 而且, 高温金属流对结晶前沿的冲刷作用, 提高了熔池中熔融金属的平衡结晶温度, 使结晶区域浓度过冷程度减小, 从而使得结晶线前沿的稳定性提高, 促进了均匀扩散, 细化凝固组织的作用效果显著[7].

由图 5 还可以看出, 当磁场电流为 5 A 时, 晶粒又变得粗大, 且出现了胞状树枝晶组织. 由于在外加磁场作用下, 磁感应强度是影响晶粒结构单元尺寸的极为重要的参数. 它们之间的关系可按文献[8] 的公式估算为

$$a=(4\pi DT_{\text{п}}/k\delta^2)\times[\gamma(\lambda_{\text{T}}+\lambda_{\text{ж}})/L\lambda_{\text{ж}}]\times 1/G_{\text{v}} \tag{1}$$

式中: $T_{\text{п}}$ 为金属熔化温度; γ 为晶体同液态金属边界上的单位自由能; λ_{T}, $\lambda_{\text{ж}}$ 为固相和液相的热传导系数; L 为金属熔化单位潜热; δ为厚度.

在较小的磁感应强度(B)的情况下, 当搅拌强度相对小时, 温度梯度(G)优先发生变化. 因此随着磁感应强度的增加, 胞晶的宽度将缩短, 并在一定的磁感应强度值时, 其宽度达到最小值. 当搅拌强度值较大时, 浓度聚集厚度将是反映胞晶尺寸的决定性参数.

由公式可知, 厚度 δ是平方值, 所以当它减少时, 尽管温度梯度在继续提高, 晶粒结构单元的宽度将增加.

图6 为镍基合金在最佳堆焊电流 140 A 和磁场电流 1 A 作用下堆焊层的显微组织. 可见, 硬质相呈长条状轴向平行于堆焊层的表面; 当硬质相呈杆状轴向垂直于被磨损表面(即为"六角形")并均匀的分布, 且材料与磨料的接触面积越少, 其受到的应力就越小, 故而能提高材料的表面耐磨性[5].

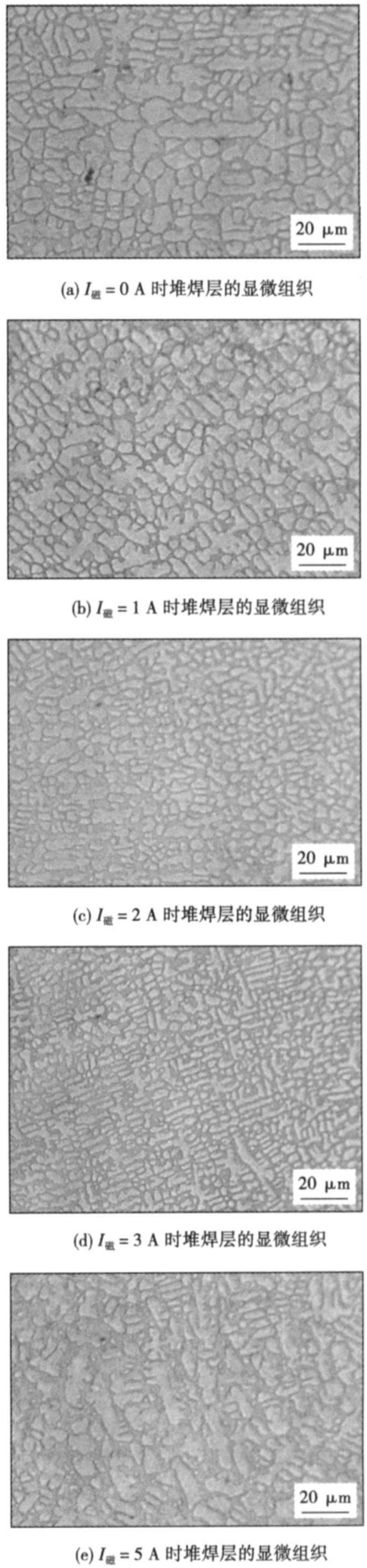

(a) $I_{\text{磁}}$ = 0 A 时堆焊层的显微组织

(b) $I_{\text{磁}}$ = 1 A 时堆焊层的显微组织

(c) $I_{\text{磁}}$ = 2 A 时堆焊层的显微组织

(d) $I_{\text{磁}}$ = 3 A 时堆焊层的显微组织

(e) $I_{\text{磁}}$ = 5 A 时堆焊层的显微组织

图 5　堆焊电流 160 A时钴基合金堆焊层的显微组织

Fig 5　Microstructures of overlay deposit at 160 A for Co-based alloy

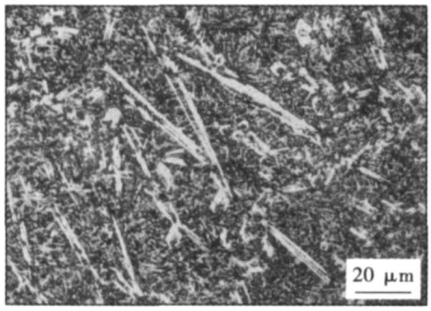

图 6 堆焊电流 140 A 时镍基合金堆焊层的表面形貌

Fig. 6 Exterior microstructures of overlay deposit at 140 A for Ni-based alloy

3 结 论

(1) 由堆焊层的金相显微组织可以得出, 只有焊接工艺参数和磁场参数相匹配的情况下, 通过电磁搅拌改变焊接熔池液态金属结晶过程中的传质和传热过程, 从而改变晶粒的结晶方向, 细化一次组织的效果最显著, 因而其硬度和耐磨性具有最佳值.

(2) 对于钴基合金, 最佳堆焊电流和磁场电流分别为 160 A, 3 A; 而镍基合金则分别为 140 A 和 1 A, 此时堆焊层的硬度和耐磨性最好; 当磁场电流继续增大时, 由于电磁阻尼占主导地位, 因而堆焊层的性能下降.

(3) 施加磁场时的堆焊层性能明显优于未施加磁场; 说明外加磁场对显微组织的细化作用和对形核率的影响效果显著, 从而使堆焊层的硬度提高, 耐磨性增强.

参考文献:

[1] 侯清宇, 高甲生. Co-Cr-W 系等离子弧堆焊合金层显微结构的研究[J]. 稀有金属材料与工程, 2004, 33(11): 1199—1202.
Hou Qingyu, Gao Jiasheng. The research of the microstructure of the Co-Cr-W alloy plasma surfacing[J]. Rare Metal Materials and Engineering, 2004, 33(11): 1199—1202.

[2] 斯松华, 何宜柱. 等离子堆焊合金层组织及腐蚀磨损性能[J]. 焊接学报, 2002, 23(2): 40—43.
Si Songhua, He Yizhu. Study on microstructures and corrosion-wear performance of plasma surfacing alloy deposits[J]. Transactions of the China Welding Institution, 2002, 23(2): 40—43.

[3] Gatto A, Bassoli E, Fornari M. Plasma transferred arc deposition of powdered high performances alloys; process parameters optimis-action as a function of alloy and geometrical configuration[J]. Surface and Coatings Technology, 2004, 187: 265—271.

[4] 阿勃拉洛夫 M A, 阿勃杜拉赫曼洛夫 P. Y. 电磁作用焊接技术[M]. 韦福水, 路登平译. 北京: 机械工业出版社, 1988.

[5] 刘政军, 程江波, 苏允海, 等. 电磁搅拌对堆焊层硬质相形态及性能的影响[J]. 热加工工艺, 2005(4): 53—55.
Liu Zhengjun, Cheng Jiangbo, Su Yunhai, *et al*. Effect of electromagnetic stirring on morphology of hard phase and property in weld metal overlay[J]. Hot Working Technology, 2005(4): 53—55.

[6] 王晓东, 赵 恂, 李廷举, 等. 磁力搅拌法的研究与开发[J]. 材料科学与工艺, 2000(12): 2—5.
Wang Xiaodong, Zhao Xun, Li Tingju, *et al*. Research and development of magnetic force agitation[J]. Materials Science and Technology, 2000(12): 2—5.

[7] 刘政军. 磁场强度对重熔层耐磨性的影响[J]. 焊接学报, 2001, 22(5): 73—75.
Liu Zhengjun. The effect of magnetic field on wear resistibility of remelted layer[J]. Transactions of the China Welding Institution, 2001, 22(5): 73—75.

[8] Hurle D T J. Interface stability during the solidification of a stirred binary-alloy melt[R]. Crystal Growth, 1969.

作者简介: 刘政军, 男, 1962 年出生, 教授, 博士研究生导师. 主要从事焊接冶金、特种焊接材料及表面强化方向的研究工作. 发表论文 60 余篇.

Email: liuzhengjun1962@163.com

MAIN TOPICS, ABSTRACTS & KEY WORDS

Study of repair welding technology of friction stir welding defects LIU Huijie[1], ZHANG Huijie[1], HUANG Yongxian[1], GUO Yongliang[2] (1. State Key Laboratory of Advanced Welding Production Technology, Harbin Institute of Technology, Harbin 150001, China; 2. Analyzing and Testing center, Harbin Institute of Technology, Harbin 150001, China). p1—4

Abstract: Welding defects can be also formed during friction stir welding under improper welding technology conditions, and the friction stir welding defects such as groove, void and kissing bond significantly influence the mechanical properties of joints. Friction stir welding process is utilized to repair these defects, and the focus is placed on the weld morphology and mechanical properties of the repaired joints. The experimental results indicated that the friction stir welding process can remove the above-mentioned welding defects, and the repaired joints have good weld morphology and excellent mechanical properties when optimum repair parameters are used. The fracture analysis showed that the repaired joints are ruptured on the retreating side of the weld in the tensile test, and the fracture surfaces are characterized by the clear plastic deformation dimples.

Key words: friction stir welding; welding defect; repair welding; weld morphology; mechanical property

Effects of different fluxes on the characteristics of Sn-Zn solders WANG Hui, XUE Songbai, CHEN Wenxue, WANG Jianxin (College of Materials Science and Technology, Nanjing University of Aeronautics and Astronautics, Nanjing 211100, China). p5—8

Abstract: The wetting characteristics of Sn-Zn solders with three different types of flux were researched by wetting balance method. Results indicated that Sn-Zn solders exhibited excellent wettability using $ZnCl_2$-NH_4Cl flux. Additionally, the spreading of Sn-9Zn solder on Cu substrate with different types of flux was investigated, and the characteristics of the intermetallic compounds (IMC) between the solder and substrate were also analyzed and compared, results showed that a flat IMC layer was present adjacent to the Cu substrate while a scallop IMC layer was close to the solder. Moreover, the characteristics of IMC and the appearances of soldered joints varied by using different fluxes. Plenty of ZnO exists on the surface of Sn-Zn solders, thus removing the ZnO is critical for the flux of Sn-Zn solders.

Key words: lead-free solder; Sn-Zn; flux; wettability

Properties of Sn-3.0Ag-0.5Cu-xNi lead-free solders and soldering joints WANG Lifeng[1,2], SUN Fenglian[2], LÜ Ye[2], SHEN Xuwei[2] (1. State Key Laboratory of Advanced Welding Production Technology, Harbin Instiute of Technology, Harbin 150001, China; 2. Harbin University of Science and Technology, Harbin 150040, China). p9—12

Abstract: The influences of the addition Nickel to Sn-3.0Ag-0.5Cu lead-free solder on the melting point, wettability, tensile properties and the properties of soldering joints were studied. The results show that the solder alloy exhibited improved wettability with the addition of small amount of Nickel. The wetting time decreases gradually and the wetting force increases gradually as Nickel content is within 0.03% ~ 0.1%. When Nickel content is 0.05% the wetting time is the shortest. When Nickel content is 0.1% the wetting force is the biggest. The solder alloy exhibited very little change on the melting point. The solder alloy of the addition of Nickel exhibited improved elongation percentage and shear strength . When Nickel content is 0.1%, the elongation percentage and shear strength are the highest. Scanning fracture exhibits obvious ductility characteristic. The suitable of addition to the solder Nickel is within 0.05% ~ 0.1%.

Key words: lead-free solder; wettability; shear strength

Arc sensor seam offset identification system based on LabVIEW and support vector regression machine ZENG Songsheng, WANG Guorong, SHI Yonghua, HUANG Guoxing (South China University of Technology, School of Mechanics and Automotive Engineering, Guangzhou 510640, China). p13—16

Abstract: The new welding seam offset identification system of arc sensor was developed with the virtual instrument LabVIEW in this paper. The data detection, wavelet filtering, data normalizing, vertical mean filtering and horizontal dimensionality reduction were depicted based on LabVIEW. The basic principle of the support vector regression machine and data-dependent kernel function was introduced. The algorithm realization of the support vector regression machine with Matlab was proposed. The design method and the control flowchart of the seam offset identification software were proposed using LabVIEW and Matlab. The experiment results confirmed that the way was feasible, the identification precision could meet the actual application in the seam tracking system.

Key words: LabVIEW; support vector regression machine; Matlab; offset identification

Microstructure and wear resistance of metal-based ceramics composite coating deposited by plasma arc surfacing LIU Zhengjun[1], ZONG Lin[1,2], SUN Jinggang[1], CI Honggang[1], SONG

Xingkui[1] (1. School of Material Science and Engineering, Shenyang University of Technology, Shenyang 110023, China; 2. School of Mechanical Engineering, Shenyang Institute of Chemical Technology, Shenyang 110142, China). p17—20

Abstract: Longitudinal magnetic field was applied on plasma arc surfacing Co-based and Ni-based alloys. Hardness, wearing and microstructures of the two ceramics composite surfacing deposit were tested in this paper. The surfacing deposit of introducing the longitudinnal magnetic field shows higher properties than the surfacing deposit without magnetic field. The properties of surfacing deposit are optimal when surfacing current is 160A and magnetic field current is 3A for Co-based alloy, the effect of grain refining for surfacing microstructure is most obvious at this time; the optimal surfacing and magnetic field currents for Ni-based alloy are 160A and 3A, and the number of hexagon ceramics hard phases of Cr_7C_3 section is most and evenly distributed. It shows that the longitudinal parallel direction of hard phases are consistent, so the hardness and wearing resistance are best. With the increasing of magnetic field current, the properties of surfacing deposit declined because electromagnetic damping play a doninant role.

Key words: plasma arc surfacing; ceramics composite; microstructure; wear resistance

Investigation on the local mechanical properties of the automobile aluminium alloy welded joint WANG Zhicheng, QIAO Jisen, CHEN Jianhong, ZHU Liang (Lanzhou University of Technology, State Key Laboratory of Gansu New Non-ferrous Metal Materials, Lanzhou 730050, China). p21—24

Abstract: Because the micro structures and mechanical properties were nonuniform in the aluminium alloy welded joint, it was necessary that the local mechanical properties was measured accurately for the assessment of the mechanical properties of whole welded joint and the improvement of the welded technique. In this paper, the micro structures and hardness of the automobile 5052 aluminium alloy were analyzed, at the same time, the small ball punch test was put forward to investigate the local mechanical properties of material which combined with a revised FEM algorithm with ABAQUS computer code. The constitutive properties of the local material was indirectly obtained by the numerical model which was a special revised iterative process and worked out the true strain-stress curves for an unknown material. The process accuracy was validated by the uniaxial tension test. The results show that the distribution character of its curve was similar with that of the welded joint hardness distribution, and the worst local mechanical properties of aluminium alloy welded joint was located around the fusion line.

Key words: welded joint; mechanical properties; small ball punch; finite element

Simulation of the microstructure evolution of welding-grain growth in heat affected zone LI Yubin, MENG Daqiao, LIU Kezhao, XIE Zhiqiang (China Academy of Engineering physics, P. O. Box 919, Mianyang 621900, China). p25—28, 32

Abstract: Based on the two factors of energy and curvature, a 2-dimension cellular automata model for simulating grain normal growth was proposed. The model can reflect some important physical phenomena on grain normal growth, including the relation of grain growth velocity to temperature and curvature and time invariance of grain size distribution. At the same time, a transition rule of cellular automata time (t_{CAS}) to real time was put forward. Energy-curvature drove cellular automata modeling normal grain growth in welding heat-affected zone is accomplished in real time. The simulation results correspond well with the rule of grain distribution in welding heat-affected zone.

Key words: cellular automata; grain growth; heat-affected zone

Local dry automatic underwater welding of 304 stainless steel ZHU Jialei[1,2], JIAO Xiangdong[2], ZHOU Canfeng[2], SHEN Qiuping[3], YU Yan[3], Gao Hui[1], DONG Jihong[1] (1. College of Mechanical and Electrical Engineering, Beijing University of Chemical Technology, Beijing 100029, China; 2. Opto-mechatronics Equipment Technology Beijing Area Major Laboratory, Beijing Institute of Petrochemical Technology, Beijing 102600, China; 3. Shanghai Nuclear Engineering Research & Design Institute, Shanghai 200233, China). p29—32

Abstract: Local dry underwater welding is one of the important techniques for its economy and flexibleness. Based on the development of local dry automatic underwater welding system, the electrical parameters of welding in air、5 meters and 15 meters under water are obtained and analyzed by using HANNOVER analysator. The results show that the welding test system can carry out local dry automatic underwater welding successfully and the metal transfer mode during underwater welding is relate to welding environment, which provide experimental foardation for analysing and assessing welding procedure and welding quality of local dry automatic underwater welding.

Key words: local dry automatic welding; hannover analysator; metal transfer

Robotic underwater weld seam tracking based on visual sensor XIAO Xinyuan, SHI Yonghua, WANG Guorong, Li Hexi (School of Mechanical Engineering, South China University of Technology, Guangzhou 510641, China). p33—36

Abstract: According to the special requirements of underwater automatic welding under environment of vision, a robotic underwater visual weld seam tracking system is developed. As underwater weld seam images are serious interference and fuzzy, wavelet transform technology is used to remove arc、splashing interference noise. An improved fuzzy enhancement image processing algorithm is adopted to improve the efficiency of image processing and obtain clear